

Evaluate and compare the antibacterial activity of lysine with curcumin and gold nanoparticles

Sheymaa S. Ismael¹, Entesar Hussein Ali², Iman Ismael Jabbar³

^{1,2,3}Division of Biotechnology, Department of science, University of Technology, Baghdad Iraq
Email: Shaaam.090@gmail.com, Entesar.H.Almosawi@uotechnology.edu.iq,
Iman.I.Alsaedi@uotechnology.edu.iq

Received: 19.09.2024

Revised: 15.10.2024

Accepted: 16.11.2024

ABSTRACT

The misuse of antibiotics directly contributes to the emergence of drug-resistant microbes. Therefore, developing innovative therapeutic approaches is crucial for addressing this issue. The rapid advancement of nanotechnology provides hope that this problem can be resolved. Consequently, conventional methods are employed to synthesize and characterize the samples. The antibacterial activity of the lysine-curcumin combination, which is a lysine-capped gold nanoparticle, was evaluated against *Staphylococcus aureus* and *Escherichia coli*. Fourier-transform infrared spectroscopy (FTIR), melting point analysis, zeta potential measurement, and UV-visible spectroscopy were used in the synthesis and characterization of curcumin, lysine, and gold nanoparticles, as well as their combinations (lysine-gold and lysine-co-curcumin). The agar-well diffusion method examined the samples' antibacterial activities against *S. aureus* and *E. coli*. Curcumin showed notable effectiveness against *S. aureus*, with inhibitory zones of up to 15 mm at 100% concentration. It shows less efficacy against *E. coli* (5 mm at 100% concentration). Lysine had significant efficacy against *S. aureus* (8 mm at 100%) but no effect on *E. coli* (4 mm at 50% and 100%). The antibacterial activity of gold nanoparticles was found to be moderate against *S. aureus* (10 mm at 100%) and restricted against *E. coli* (2 mm at 100%). Remarkably, the combination of lysine and gold nanoparticles enhanced antibacterial effectiveness, resulting in inhibition zones of 14 mm for *S. aureus* and 8 mm for *E. coli* at 100%. Similarly, Lysine-Co-Curcumin exhibited high activity against *S. aureus* (14 mm at 100%) and *E. coli* (6 mm at 100%).

Keywords: *S. aureus*, *E. coli*, gold nanoparticles, curcumin, FTIR.

INTRODUCTION

The primary worldwide health concern is the emergence of drug-resistant microorganisms. Multidrug-resistant bacteria is considered a public health problem globally [1]. *Staphylococcus aureus* is the most prevalent bacterium resistant to medications and capable of transmission between humans and animals, posing a severe risk to human well-being [2]. This bacterium is responsible for various illnesses such as bacteremia, endocarditis, pneumonia, and chronic osteomyelitis, and can affect multiple organs and tissues [3]. Additionally, *Escherichia coli* (*E. coli*) is a common component of the normal gut microbiota in humans and animals, characterized by its high adaptability. This bacterium, which is typically harmless and resides as a commensal organism, can evolve into a pathogen by acquiring mobile genetic elements containing virulence genes. Consequently, it can cause a wide array of diseases both within and beyond the gastrointestinal tract [4].

There is considerable promise for the advancement of antibacterial therapy through the utilization of delivery systems based on nanomaterials [5], whether these systems serve as active agents or drug carriers [6]. For instance, metal nanoparticles and nanomaterials derived from graphene exhibit inherent antibacterial properties that can be triggered through physical disruption or phototherapy [7]. These antimicrobial functional nanoparticles do not inherently induce bacterial resistance [8]. When employed as drug carriers, nanomaterials can impede bacterial resistance mechanisms by evading drug-resistant processes while safeguarding the essential structural components of the loaded antibiotics, such as the beta-lactam ring. Furthermore, by enhancing drug targeting precision, improving drug pharmacokinetics, and promoting interactions with bacteria, nanomaterials have the potential to enhance the antibacterial efficacy of medications [9].

This study synthesized and characterized gold nanoparticles capped with lysine to explore their antibacterial properties. Additionally, the research investigated the antibacterial effects of the lysine-capped gold nanoparticles and the lysine-curcumin complex on *S. aureus* and *E. coli* bacteria.

MATERIALS AND METHODS

Lysine-produced *S. aureus* was previously isolated from the wound infection of the patient and incubated in the shaker at 110 rpm at 37 °C, pH 7, for 72 hours to produce lysine. The primary method for producing lysine is the use of chosen isolation. This involves a multi-step process that includes fermentation, centrifugation to separate the cells, product separation[10], and purification[11].

UV-VIS spectroscopy[12], FTIR[13], melting point[14], and zeta potential[15] were used to characterize the lysine-capped gold nanoparticles, curcumin, and curcumin-lysine complex.

The antibacterial properties of the generated materials (curcumin, lysine, gold, lysine-gold, and lysine-Co-curcumin) were assessed against strains of Gram-positive and Gram-negative bacteria using the agar well diffusion test [16, 17]. Aseptic inoculation of sterile Petri dishes was performed using 20 millilitres of Muller-Hinton (MH) agar. The bacterial species were taken out of their stock cultures using a sterile wire loop. After the organisms were cultivated, 6 mm-diameter wells were punched onto the agar plates using a sterile needle. The bored wells were filled with various concentrations of the samples. The cultured plates holding the samples and test organisms were measured, and the average width of the zones of inhibition was recorded after they were incubated at 37 °C for the entire night[18, 19].

Lysine-capped gold nanoparticles exhibit a melting point above 1000°C. Lysine, a bifunctional amino acid, interacts strongly with the gold surface through its amino and carboxyl groups, forming a robust protective layer that significantly reduces the surface energy and enhances thermal stability.

The successful production of lysine-capped gold nanoparticles was verified by the noticeable shift in colour from pink to dark pink during an overnight ageing period. L-lysine was dissolved in purified water to a concentration of 1 mM and mixed with gold solution; the pH was adjusted to 10, and the mixture was allowed to age at room temperature. The purification through multiple centrifugation steps with distilled water effectively removed impurities, yielding sediment rich in lysine-capped gold nanoparticles. This simple yet effective method highlights the feasibility of using amino acids as capping agents, potentially expanding applications in biomedicine, catalysis, and material science. Further characterization of these nanoparticles will provide detailed insights into their structural and surface properties.

The synthesis of lysine-curcumin (cur_lys) was successfully achieved through the reflux of curcumin and lysine in an ethanolic solution with a small amount of glacial acetic acid, maintained at 55–60 °C for 5 hours. After that, the reaction mixture was concentrated to a third of its initial volume, producing a precipitate with a dark yellow color. The sample was dried over fused calcium chloride after filtering and cleaning with ethanol. Recrystallization from ethanol produced a brown solid product with a mass of 1.5 g, indicating a high yield. The successful formation of the dark yellow product, distinct from the initial white lysine and yellow curcumin, suggests that the desired chemical reaction occurred efficiently. The color change and solid state of the products are consistent with the expected properties of a lysine-curcumin complex, demonstrating the effectiveness of the synthesis method.

The lysine-curcumin-cobalt complex was synthesized successfully to yield a dark yellow product with a mass of 0.5 g after drying at 30 °C. The reaction involved refluxing $\text{CoCl}_2 \cdot 6\text{H}_2\text{O}$ with lysine-curcumin in ethanol for 5 hours, followed by volume reduction, cooling, and filtration. The sample was thoroughly washed with ethanol and recrystallized, resulting in the desired complex. The dark yellow color and solid state of the product indicate the successful complexation of cobalt with lysine-curcumin. This confirms the effectiveness of the synthesis method and the stability of the resulting Schiff base complex.

RESULT AND DISCUSSION

The peaks in the FTIR spectra of lysine-capped gold nanoparticles show the functional groups that are present and how they interact with the gold surface (Figure 1). O-H stretching vibrations correlate with the highest peak at 3328 cm^{-1} , indicating the presence of hydroxyl groups, possibly from lysine or water [20]. C-H stretching vibrations are responsible for the signal at 2788 cm^{-1} , which suggests aliphatic structures in lysine [21]. The highest peak at 1635 cm^{-1} indicated by N-H bending vibrations, which are essential for stabilizing the nanoparticles and corroborating the existence of primary amines from lysine [22]. The peak at 899 cm^{-1} due to C-N stretching vibrations further supports the presence of amine groups. The lower frequency peaks at 546 cm^{-1} and 512 cm^{-1} likely indicate metal-ligand interactions, essential for nanoparticle stability. These observations confirm the successful capping of gold nanoparticles with lysine, providing stability and preventing aggregation.

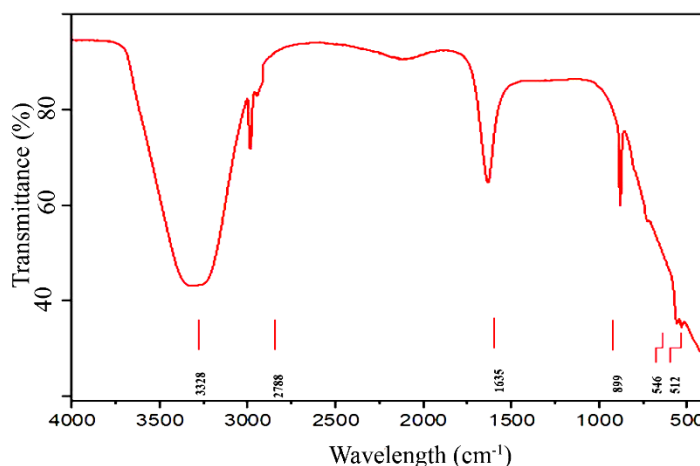


Figure 1: The FTIR of lysine capped gold nano-film

The UV-VIS of lysine capped with gold nano-film

The UV-VIS characterization of lysine with gold nanoparticles revealed that the reaction between lysine and gold nanofilm significantly influences their electronic environment and absorbance properties, as observed through UV-VIS spectroscopy. The study results revealed that a peak at 528.42 nm confirms the presence of gold nanoparticles and their interaction with lysine, as presented in Figure 2. The lysine-gold nanofilm's significant peak at 528 nm was reported [23].

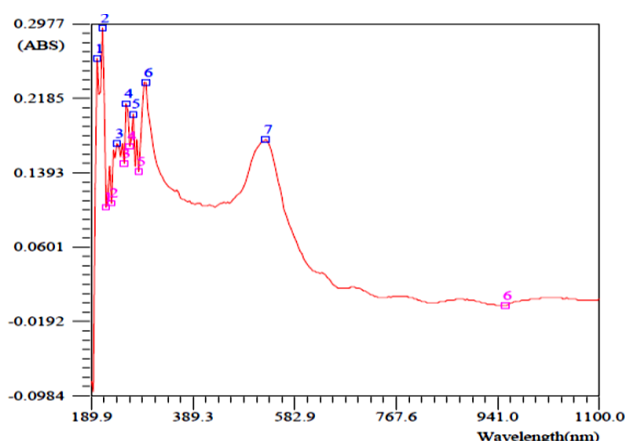


Figure 2: UV-VIS of lysine covered with gold nanofilm

A transverse band with a range between 567–574 nm was seen in the absorption spectra of amino acid threonine capped with gold nanoparticles by Swami et al.[24]. Lysine has no effect on the UV-vis spectra of gold nanoparticle solutions, as demonstrated by A. Mocanu et al., which contrasts with other nanoparticles like cysteine that have a significant effect on them. The λ_{max} 546 of the lysine-gold nanoparticles was reported [25]. A. Tsalsabilaet al. found the UV-VIS spectra of lysine-capped gold nanoparticles demonstrated stable absorption peaks over time, with the maximum absorbance remaining at 507.07 nm even after thirty days, showing that lysine provides a stable capping layer that prevents nanoparticle aggregation [26]. O. Horovitz et al. indicated a diluted 0.01 M lysine solution has a low modification in the UV-VIS spectrum of the gold nanoparticle solution with λ_{max} between 528 and 530 nm [27].

These results demonstrate that gold nanoparticles and lysine interact significantly, changing the absorbance characteristics of the latter and suggesting stable, well-dispersed colloids. The reason why amine-rich amino acids such as arginine (Arg) and lysine (Lys) in modified gold (Au) nanoparticles flocculate is due to interactions between the amino acids attached to the nanoparticle surface. The side chain amino groups frequently bind to the Au nanoparticle surface. The terminal amino group forms hydrogen bonds with the carboxyl group of another amino acid on a nearby nanoparticle. This interaction helps the nanoparticles aggregate or flocculate.

The zeta potential of Lysine capped gold nanoparticles

The result of Zeta potential for Lysine capped gold nanoparticles was -45 mV indicating a stable negative charge on their surface. The zeta potential of gold nanoparticles in this study was -38. When added of lysine to gold nanoparticles the Zeta potential becomes even more negative reaching -45 mV as shown in Figure 3. The rise in negative charge implies that particles resist each other more strongly resulting in better colloidal stability and less aggregation. The lysine modification exhibits influence on the structure and stability of gold nanoparticles in suspension which is vital for a variety of applications in nanotechnology and biomedicine. The zeta potential of lysine-capped gold nanoparticles was found by A. Tsalsabila et al. to be about -35.0 ± 0.8 mV, indicating increased suspension stability and longer life due to the repulsive forces preventing nanoparticle aggregation[26]. Lysine-capped gold nanoparticles were found to have a zeta potential of -21.5 mV[27].

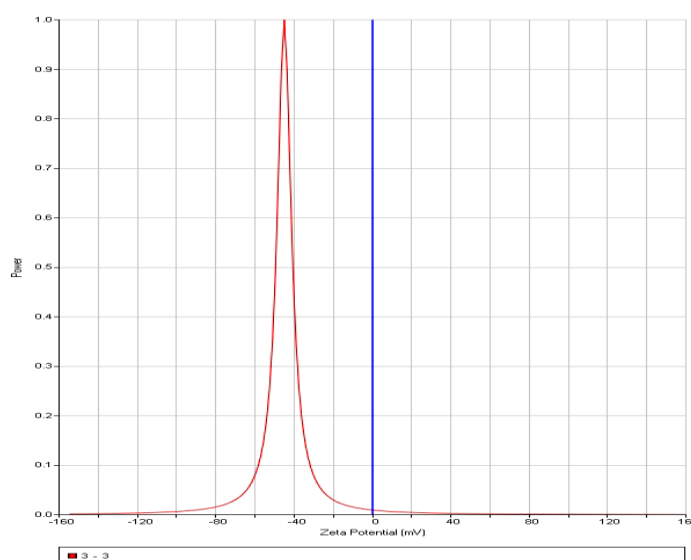


Figure 3: The zeta potential of lysine capped gold nanoparticle

Characterization of curcumin- The FTIR of curcumin

Curcumin's FTIR data shows different peaks at wavenumbers, indicating the presence of crucial functional groups inside the molecule as shown in Figure 4. Notable peaks are produced at 419 cm^{-1} , 457 cm^{-1} , and 472 cm^{-1} by aromatic ring bending vibrations [28]. Peaks at 1044 and 1086 cm^{-1} resulted from phenolic and methoxy groups' C–O stretching vibrations [29]. Additionally, for C=O stretching in α , β -unsaturated carbonyl groups, 1636 cm^{-1} to 1652 cm^{-1} [30].

Additionally, peaks at 3356 cm^{-1} and 3566 cm^{-1} indicate O–H stretching vibrations indicating the presence of hydrogen-bonded and free hydroxyl groups[31]. These results validate the complex molecular structure of curcumin, which includes aromatic rings, methoxy, phenolic, carbonyl, and hydroxyl groups that support its bioactive capabilities and applicability in diverse sectors.

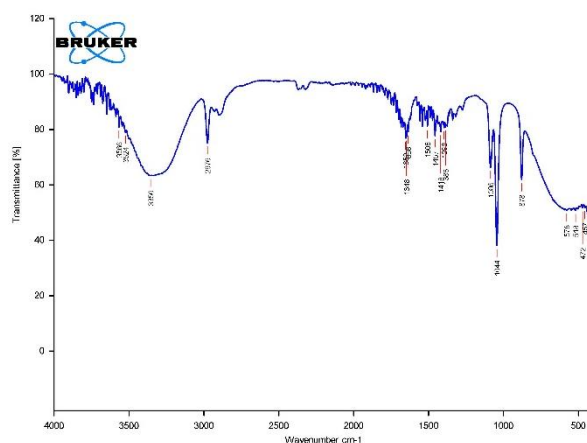


Figure 4:The FTIR analysis spectra of curcumin

The UV-VIS spectrophotometry of curcumin was performed using a dual-beam spectrophotometer which stated the significant absorbance peak at 406.92 nm and 441.94 nm with an absorbance value reach to 4.500 ABS. The current study aligns with findings of previous studies properties of curcumin. Due to its conjugated double bond structure, curcumin, a naturally occurring polyphenol obtained from the rhizome of *Curcuma longa*, could absorb ultraviolet light as shown in Figure 5. It has demonstrated similar spectroscopic characteristics with an absorption maximum observed at 441 nm[32], while others reported a peak at nearly 425 nm[33]. It has been found the spectral scan λ_{\max} of curcumin to be at 421 nm[34].

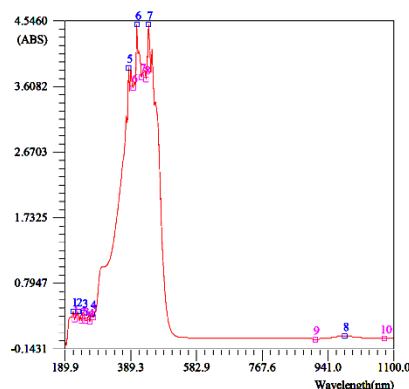


Figure 5: UV-VIS spectrophotometry of curcumin

Curcumin's characteristic conjugated system was supported by the existence of absorption maxima at 520 nm in acetone-bicarbonate buffer (pH 11) [35], demethoxycurcumin and bis-demethoxycurcumin showed that curcumin's highest absorption wavelength in a variety of polar solvents and surfactant solutions is about 430 nm[36], whereas 424 nm was the maximum curcumin absorbance in methanol that was measured[37]. Y. B. Murti et al. conducted a detailed UV-VIS spectroscopic analysis of curcumin and piperine mixtures. They reported a maximum absorbance for curcumin at 430 nm in a dissolution medium composed of sodium lauryl sulfate and phosphate buffer, further confirming curcumin's characteristic UV absorption properties. The investigation confirmed the limits of detection (LOD), limit of quantification (LOQ), specificity, linearity, accuracy, and precision of the method. These findings are consistent with the current study's results, showing maximum absorbance at 406.92 nm and 441.94 nm. This consistency across various studies emphasizes curcumin's strong UV-absorbing properties[38].

The curcumin sample demonstrated a melting point of 183°C, which is consistent with its known thermal properties. This melting point is indicative of the purity and crystalline structure of the curcumin.

The lysine-curcumin complex exhibited a melting point was 191°C which reflects the thermal stability of the complex. This melting point is higher than curcumin alone which has a melting point 183°C indicating that the formation of the complex with lysine modifying the thermal properties of curcumin. The increased melting point suggests enhanced stability due to the interaction between lysine and curcumin potentially leading to a more robust structure.

The lysine-curcumin-cobalt complex exhibited a melting point of 218°C. This elevated melting point, compared to the individual melting points of lysine (215°C) and curcumin (183°C), suggests a significant increase in thermal stability due to the formation of the complex. The interaction between lysine, curcumin, and cobalt likely results in a more robust and thermally stable structure.

FTIR of lysine-curcumin complex

The lysine-curcumin complex's FTIR spectrum is shown in Figure (6). It displays distinct absorption peaks that are indicative of various vibrational modes of the functional groups that make up the complex. The C-N bond's bending vibrations are represented by the peak at 466 cm^{-1} , while the C-S bond's stretching vibrations are indicated by the peaks at 619 cm^{-1} and 647 cm^{-1} . The out-of-plane bending vibrations of the C-H are indicated by the peak at 927 cm^{-1} . The C-O stretching vibrations corresponding to the peaks at 1020 cm^{-1} , 1127 cm^{-1} , and 1158 cm^{-1} show either or hydroxyl groups. The presence of amine groups is shown by the absorption at 1221 cm^{-1} and 1256 cm^{-1} , which is caused by C-N stretching vibrations. The vibrations of C-H bending are linked to the peaks at 1343 cm^{-1} and 1405 cm^{-1} . The carboxylate group's conspicuous peak at stretching frequencies of 1555 cm^{-1} [39].

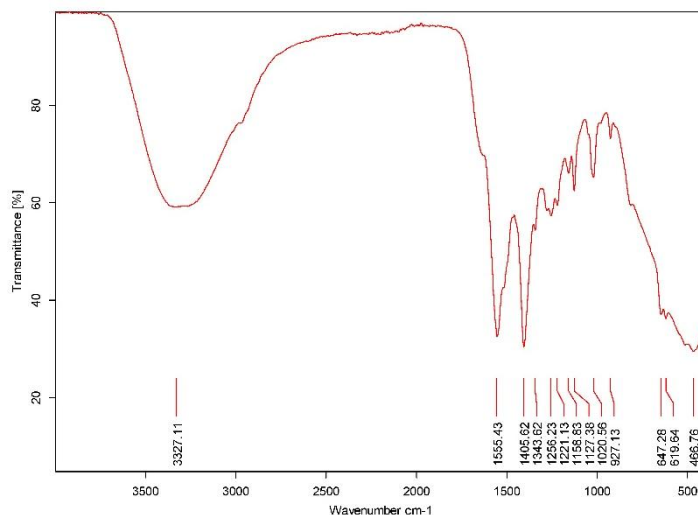


Figure 6: The FTIR spectrum of the lysine-curcumin complex

The UV-VIS characterization of the lysin-curcumin complex demonstrated significant absorbance properties, particularly with a maximum absorbance (λ_{max}) at 399.93 nm and a high absorbance value of 4.5000 ABS. This peak indicates strong interaction between lysin and curcumin, likely due to electronic transitions within the complex figure (7).

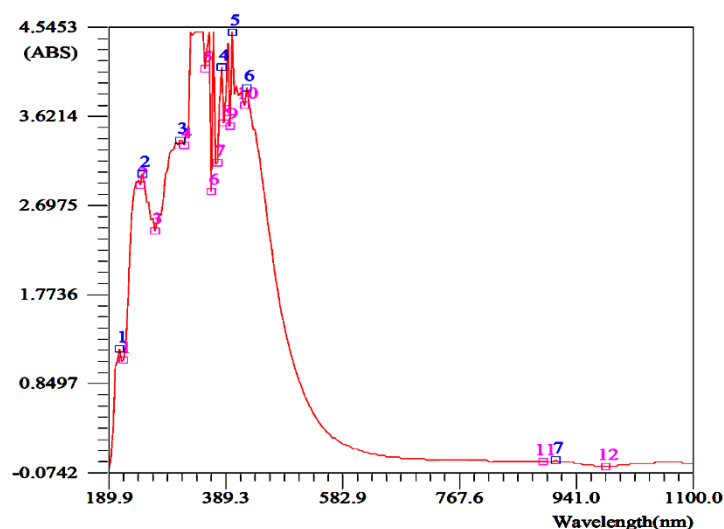


Figure 7: The UV-VIS of lysin-curcumin

FTIR of the lysine-curcumin-cobalt

The FTIR spectrum of the lysine-curcumin-cobalt nanoparticles displays distinct absorption peaks, each corresponding to various vibrational modes of functional groups within the complex as shown in Figure 8. The peak at 491.85 cm^{-1} suggests metal-ligand interactions, specifically involving cobalt with oxygen or nitrogen atoms. C-S stretching vibrations are attributed to the peaks at 648.08 cm^{-1} and 840.96 cm^{-1} , suggesting the presence of sulfur-containing molecules in the structure. The peaks at 1072.42 cm^{-1} and 1124.5 cm^{-1} are linked to C-O stretching vibrations that may indicate the existence of ether or hydroxyl groups. The peak at 1564.27 cm^{-1} is linked to C=C stretching vibrations, typical of aromatic rings in curcumin, while the peaks at 1408.04 and 1489.05 cm^{-1} are correlated with C-H bending vibrations. The presence of alkyl chain C-H stretching vibrations is shown by the high peak at 2889.37 cm^{-1} . The peaks at 3444.87 cm^{-1} and 3755.4 cm^{-1} , which indicate the presence of hydroxyl groups from lysine or curcumin, are indicative of O-H stretching vibrations. These results point to intricate interactions involving amines, hydroxyls, ethers, sulfur-containing groups, and aromatic rings between lysine, curcumin, and cobalt ions that support the stability and activity of the nanoparticles.

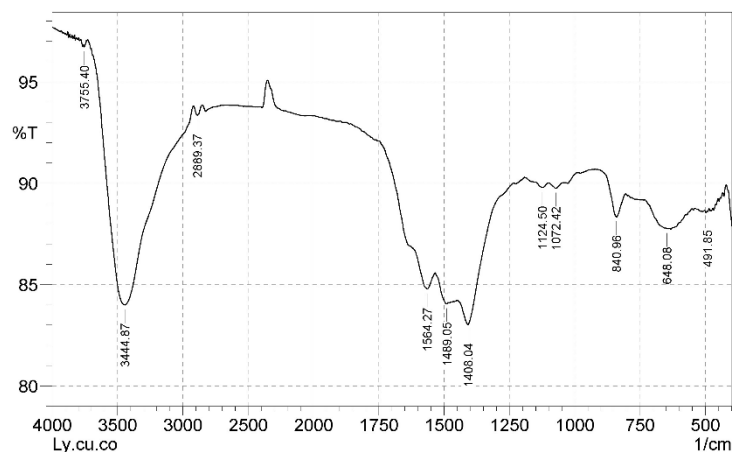


Figure 8: FTIR analysis spectra of the lysine-curcumin-cobalt

The UV-VIS spectroscopy analysis of the lysine-curcumin-cobalt complex, conducted using a MetertechUVmate spectrophotometer, revealed significant absorption peaks at 354.13 nm (0.9090 ABS), indicating strong electronic transitions due to $\pi-\pi^*$ and $n-\pi^*$ interactions within the complex (Figure 9).

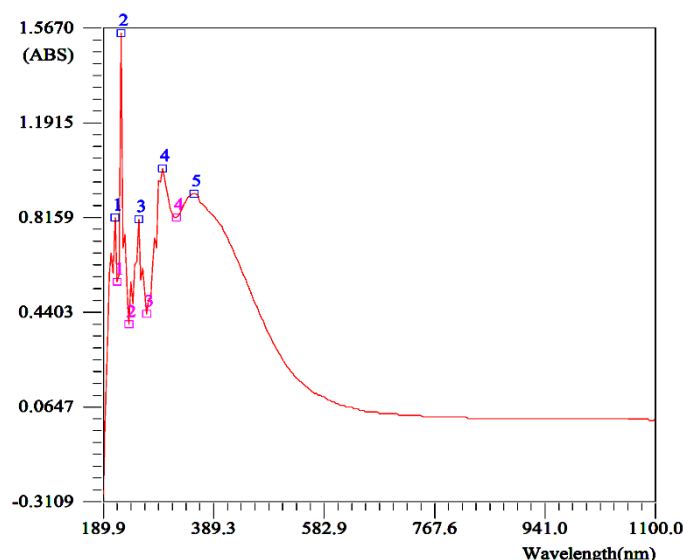


Figure 9: UV-VIS spectroscopy analysis of the lysine-curcumin-cobalt complex

Synergistic effects of Curcumin, Lysine, and Gold Nanoparticles

In this work, the agar well diffusion method was used to examine the antibacterial activity of curcumin, lysine, and gold nanoparticles, as well as their combinations (Lysine-Gold and Lysine-Co-Curcumin), against *S. aureus* and *E. coli*. Figure 10 illustrates how curcumin was less effective (5 mm at 100% concentration) against *E. coli* but shown strong action against *S. aureus*, with inhibition zones reaching 15 mm at 100% concentration. Curcumin extract antimicrobial susceptibility tests against *S. aureus* ATCC 6571 yielded similar results, with clinical isolates demonstrating strong activity against both standard and clinical isolates, with zones of inhibition ranging from 9 to 21 mm [40]. G. Kasta reported inhibition zones of curcumin at concentration 25mg/ml were 7.03 and 7.23 for *S. aureus* and *E. coli*, respectively [41]. S. S. Hettiarachchiet al. reported inhibition zones for *S. aureus* at 24.82 ± 0.54 mm, while for *E. coli*, the zones were 19.70 ± 1.18 mm [42]. S. Mukhtar found the inhibition zone of *E. coli* to be 10 ± 0.38 mm for aqueous curcumin extract and 11 ± 0.42 mm for ethanolic curcumin extract [43] and these results also correlate with another study [44]. Gram-positive (*Streptococcus mutans*) and Gram-negative (*E. coli* and *Pseudomonas aeruginosa*) bacteria are both considerably inhibited in their growth by curcumin.

According to Figure 11, lysine had little effect on *E. coli* (4 mm at 50% and 100%) and moderate activity against *S. aureus* (8 mm at 100%), which is consistent with other research on its effectiveness against Gram-positive bacteria. Li et al. [45]. reported the widths of the inhibition zones of *S. aureus* (12 ± 0.1 mm) and *E. coli*

(10 ± 0.5 mm) treated with 200 mg/ml of lysine. They showed that the minimum inhibitory concentration of lysine against both *S. aureus* and *E. coli* was 12.5 mg/ml. Furthermore, the examination of the bacterial cells under test using scanning electron microscopy demonstrated that lysine significantly altered their shape. Z. Tan et al. resulted in a high concentration of lysine that might cause significant damage to the peptidoglycan in the *S. aureus* cell wall, making the cell wall more brittle [46]. According to A. Vibhute et al., lysine has antibacterial action against *S. aureus* and *E. coli*, with an inhibition zone ranging from 7 to 20 mm [47].

As shown in figure 12, gold nanoparticles demonstrated moderate antibacterial effects, particularly against *S. aureus* (10 mm at 100%), with minimal impact on *E. coli* (2 mm at 100%), corroborating previous findings on their effectiveness against Gram-positive bacteria. This result agreement with [48] found the antibacterial activity of AuNPs against *E. coli* was 5 to 9 mm and against *S. aureus* was 3 to 11 mm. S. M. Vidya et al. showed that the AuNPs' antibacterial action is achieved by lowering ATPase activity, compressing the membrane potential, and preventing tRNA from binding to ribosomal subunits.

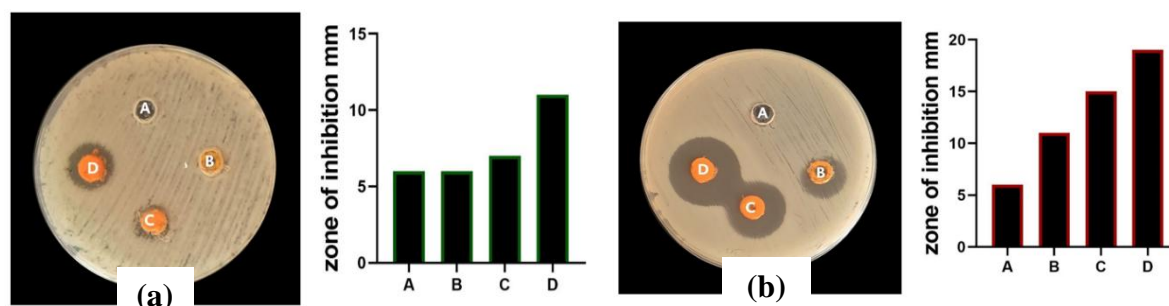


Figure 10: Antibacterial action of Curcumin with (a) *E. coli* and (b) *S. aureus*. where A) Control, B) 25%, C) 50%, and D) 100%.

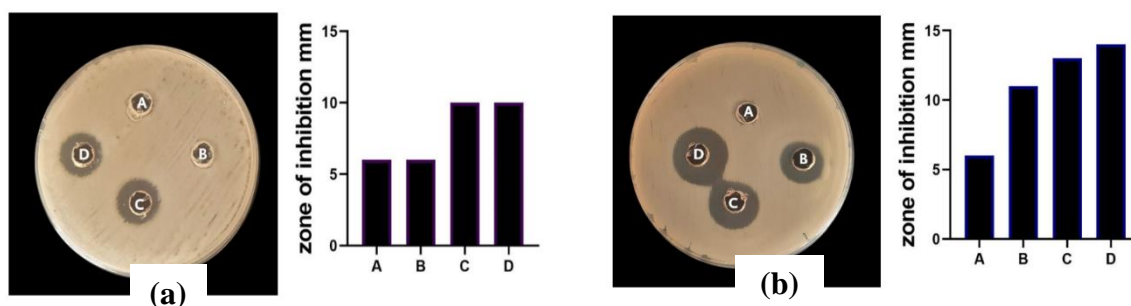


Figure 11: Antibacterial activity of Lysine with (a) *E. coli* and (b) *S. aureus*. where A) Control, B) 25%, C) 50%, and D) 100%.

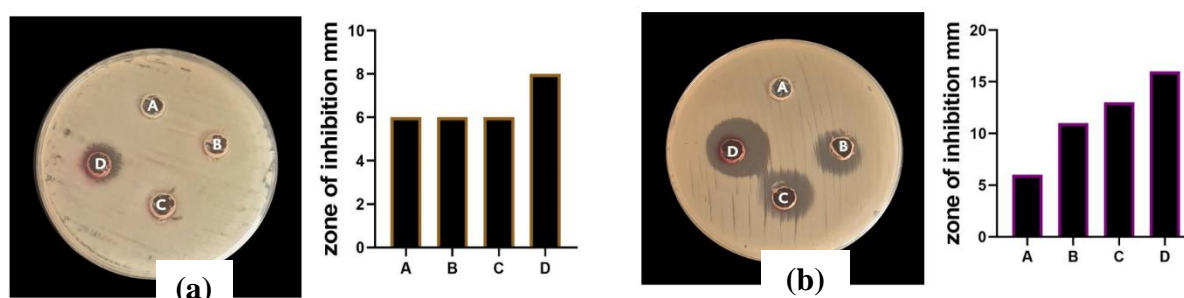


Figure 12: Antibacterial activity of (Gold) with (a) *E. coli* and (b) *S. aureus*. where A) Control, B) 25%, C) 50%, and D) 100%.

Notably, the lysine and gold nanoparticles combination enhanced antibacterial efficacy figure 13 showing inhibition zones of 14 mm for *S. aureus* and 8 mm for *E. coli* at 100%, suggesting a synergistic effect supported by earlier research. The study result agreement with [49] which concluded that AuNPs do not have any antibacterial activity toward *E. coli* but with lysine functionalized AuNPs have significant antibacterial activity due to the presence of lysine helps in initial electrostatic attractions and cell wall lysis. Similarly, Lysine-Co-Curcumin showed strong activity against *S. aureus* (14 mm at 100%) and improved activity against *E. coli* (6 mm at 100%), indicating enhanced efficacy over individual components as shown in figure 14. These results

highlight the potential of combination therapies in enhancing antibacterial activity, likely through synergistic mechanisms that increase bacterial cell membrane disruption or interfere more effectively with bacterial metabolism. The study underscores the potential of these nanoparticles, particularly in combination, as effective antimicrobial agents, especially against Gram-positive bacteria, paving the way for the development of new antibacterial treatments.

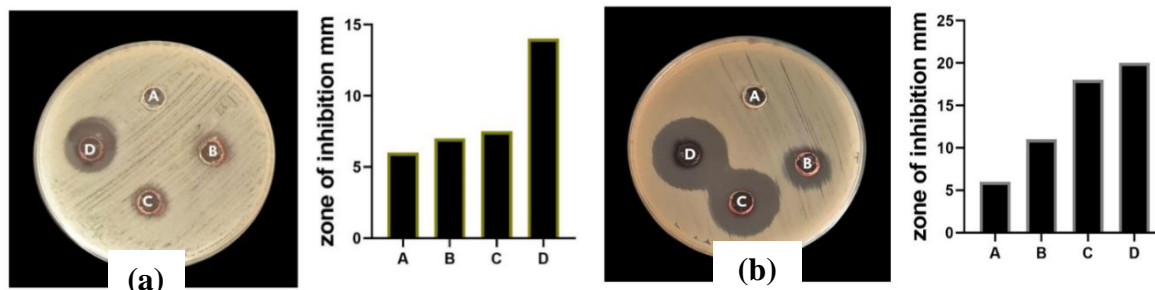


Figure 13: Antibacterial activity of (Lysine-Gold) with (a) *E. coli* and (b) *S. aureus*. where A) Control, B) 25%, C) 50%, and D) 100%.

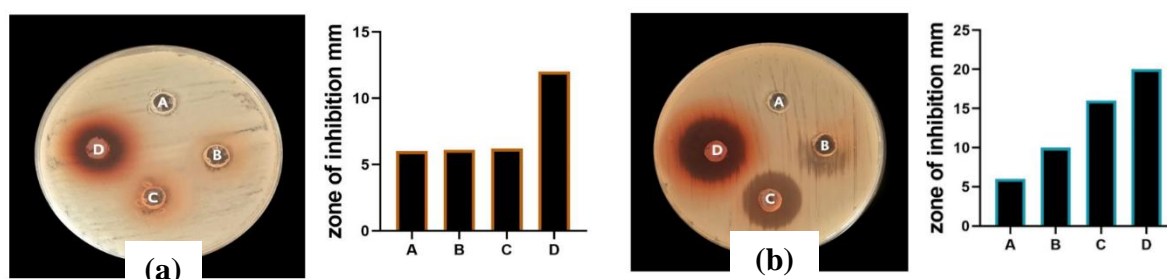


Figure 14: Antibacterial activity of (Lysine-Co- Curcumin) with (a) *E. coli* and (b) *S. aureus*. where A) Control, B) 25%, C) 50%, and D) 100%.

CONCLUSION

Research suggests that different combinations of curcumin, lysine, and gold nanoparticles have different levels of antibacterial action against *S. aureus* and *E. coli*. It is possible that these chemicals have shown activity in reducing the proliferation or survival of various bacterial varieties. Overall, the research highlights the potential of these compounds in the field of antimicrobial research and points towards the need for further exploration and development in this area.

ACKNOWLEDGEMENT

Our deepest appreciation goes out to everyone who helped bring this study to fruition.

Conflict of interest

Authors have no conflicts of interest.

REFERENCES

- Kadhim, A. S., Jasim, B. H., & Ghadir, G. K. "Antibacterial activity of *Klebsiella pneumoniae* isolated from pneumonia patients." *Journal of Emergency Medicine, Trauma & Acute Care* 6, 2024, doi:https://doi.org/10.5339/jemtac.2024.absc.18.
- Omran ZH, Hussien AK, Yahya AM, Mohammed DA, Rawdhan HA, Ahmed HM, Sattar RJ, Hussien YA, Jasm BH, Sadoon NM. "Copper Nanoparticles Against Two Types of Bacteria *Staphylococcus Aureus* and *Escherichia Coli*." *Journal of Nanostructures*, vol.14, no.3, p.780-788, 2024, doi:10.22052/JNS.2024.03.008.
- V. Silva, S. Correia, J. E. Pereira, G. Igrejas, and P. Poeta, "Surveillance and Environmental Risk Assessment of Antibiotics and AMR/ARGs Related with MRSA: One Health Perspective," 2020.
- B. Pakbin, W. M. Brück, and J. W. A. Rossen, "Virulence Factors of Enteric Pathogenic *Escherichia coli*: A Review," (in eng), *Int J Mol Sci*, vol. 22, no. 18, Sep 14 2021, doi: 10.3390/ijms22189922.
- H. J. Mohamad, Y. M. Abdul-Husain, and U. A. S. Al-Jarah, "The structural, optical, and morphological properties of NiO-Cu prepared by spray pyrolysis technique," *Microwave and Optical Technology Letters*, vol. 62, no. 11, pp. 3519-3526, 2020/11/01 2020, doi: https://doi.org/10.1002/mop.32500.

6. H. J. Mohamad, S. H. Kafi, and D. A. Taban, "Ag/CdS Surface Plasmon Simulation Systems for Gas Sensor," *Kuwait Journal of Science*, 2023.
7. Y. Gao, Y. Chen, Y. Cao, A. Mo, and Q. Peng, "Potentials of nanotechnology in treatment of methicillin-resistant *Staphylococcus aureus*," *European Journal of Medicinal Chemistry*, vol. 213, p. 113056, 2021/03/05/ 2021, doi: <https://doi.org/10.1016/j.ejmech.2020.113056>.
8. Abdula, Ahmed Mutanabbi, Ghosoun Lafta Mohsen, Bilal H. Jasim, Majid S. Jabir, Abduljabbar IR Rushdi, and Younis Baqi. "Synthesis, pharmacological evaluation, and in silico study of new 3-furan-1-thiophene-based chalcones as antibacterial and anticancer agents." *Heliyon* (2024),doi:10.1016/j.heliyon.2024.e32257.
9. M. A. Bazán Henostroza et al., "Antibiotic-loaded lipid-based nanocarrier: A promising strategy to overcome bacterial infection," *International Journal of Pharmaceutics*, vol. 621, p. 121782, 2022/06/10/ 2022, doi: <https://doi.org/10.1016/j.ijpharm.2022.121782>.
10. G. Zhou et al., "Research on a novel poly (vinyl alcohol)/lysine/vanillin wound dressing: Biocompatibility, bioactivity and antimicrobial activity," *Burns*, vol. 40, no. 8, pp. 1668-1678, 2014/12/01/ 2014, doi: <https://doi.org/10.1016/j.burns.2014.04.005>.
11. A. Sousa, F. Sousa, and J. A. Queiroz, "Impact of lysine-affinity chromatography on supercoiled plasmid DNA purification," *Journal of Chromatography B*, vol. 879, no. 30, pp. 3507-3515, 2011/11/15/ 2011, doi: <https://doi.org/10.1016/j.jchromb.2011.09.032>.
12. Sattar, Rand Jabbar, and Entesar Hussain Ali. "Purification and Characterization of Lipase Production from *Pseudomonas Aeruginosa* and Study Effect of Silver Nanoparticle in Activity of Enzyme in Application of Biology." *Plant Arch*, vol. 19, no. 2, p. 4379-85, 2019.
13. K. Ahire, D. Kumar, and A. Ali, "Differential glycation of arginine and lysine by glucose and inhibition by acesulfame potassium," *Journal of BioScience and Biotechnology*, vol. 7, pp. 11-15, 2018.
14. E. V. Lukasheva, M. G. Makletsova, A. N. Lukashev, G. Babayeva, A. Y. Arinbasarova, and A. G. Medentsev, "Fungal Enzyme L-Lysine α -Oxidase Affects the Amino Acid Metabolism in the Brain and Decreases the Polyamine Level," (in eng), *Pharmaceuticals (Basel)*, vol. 13, no. 11, Nov 17 2020, doi: 10.3390/ph13110398.
15. A. Serrano-Lotina, R. Portela, P. Baeza, V. Alcolea-Rodriguez, M. Villarroel, and P. Ávila, "Zeta potential as a tool for functional materials development," *Catalysis Today*, vol. 423, p. 113862, 2023/11/01/ 2023, doi: <https://doi.org/10.1016/j.cattod.2022.08.004>.
16. Nafea MH, Kadhim AJ, Obayes KR, Jasim BH, Hasan AF. Biosynthesis of TiO_2 Nanoparticles using and Evaluation of their Antibacterial Activities. *Journal of Bioscience and Applied Research*, "vol. 11, 2025.
17. Ali, Entesar H., and Karrar R. Mohammed. "Extraction, purification and characterization of peroxidase from *pseudomonas aeruginosa* and utility as antioxidant and anticancer." *Baghdad Sci J* vol. 16, no. 4 ,2019.
18. M. A. Jihad, F. T. M. Noori, M. S. Jabir, S. Albukhaty, F. A. AlMalki, and A. A. Alyamani, "Polyethylene Glycol Functionalized Graphene Oxide Nanoparticles Loaded with *Nigella sativa* Extract: A Smart Antibacterial Therapeutic Drug Delivery System," (in eng), *Molecules*, vol. 26, no. 11, May 21 2021, doi: 10.3390/molecules26110367.
19. Jasim, B. H., and E. H. Ali. "Isolation, extraction, purification, and characterization of fibrinolytic enzyme from *Pseudomonas aeruginosa* and estimation of the molecular weight of the enzyme." *Archives of Razi Institute* 76, no. 4, p. 809-820, 2021, doi: 10.22092/ari.2021.355745.1716.
20. N. Wangoo, K. K. Bhasin, S. K. Mehta, and C. R. Suri, "Synthesis and capping of water-dispersed gold nanoparticles by an amino acid: bioconjugation and binding studies," (in eng), *J Colloid Interface Sci*, vol. 323, no. 2, pp. 247-54, Jul 15 2008, doi: 10.1016/j.jcis.2008.04.043.
21. C. Malarkodi, S. Rajeshkumar, M. Vanaja, K. Paulkumar, G. Gnanajobitha, and G. Annadurai, "Eco-friendly synthesis and characterization of gold nanoparticles using *Klebsiella pneumoniae*," *Journal of Nanostructure in Chemistry*, vol. 3, no. 1, p. 30, 2013/05/08 2013, doi: 10.1186/2193-8865-3-30.
22. S. Randhawa, A. I. Dar, T. C. Saini, M. Bathla, and A. Acharya, "Glucosamine conjugated gold nanoparticles modulate protein aggregation induced autophagic neuronal cell death via regulation of intracellular Parkin homeostasis," *Nano Today*, vol. 56, p. 102243, 2024/06/01/ 2024, doi: <https://doi.org/10.1016/j.nantod.2024.102243>.
23. E. J. Yoo, T. Li, H. G. Park, and Y. K. Chang, "Size-dependent flocculation behavior of colloidal Au nanoparticles modified with various biomolecules," *Ultramicroscopy*, vol. 108, no. 10, pp. 1273-1277, 2008/09/01/ 2008, doi: <https://doi.org/10.1016/j.ultramic.2008.04.051>.
24. A. Swami, S. Mittal, A. Chopra, R. K. Sharma, and N. Wangoo, "Synthesis and pH-dependent assembly of isotropic and anisotropic gold nanoparticles functionalized with hydroxyl-bearing amino acids," *Applied Nanoscience*, vol. 8, pp. 467-473, 2018.
25. A. Mocanu, I. Cernica, G. Tomoaia, L.-D. Bobos, O. Horovitz, and M. Tomoaia-Cotisel, "Self-assembly characteristics of gold nanoparticles in the presence of cysteine," *Colloids and Surfaces A:*

- Physicochemical and Engineering Aspects, vol. 338, no. 1, pp. 93-101, 2009/04/15/ 2009, doi: <https://doi.org/10.1016/j.colsurfa.2008.12.041>.
26. A. Tsalsabila, Y. Herbani, and Y. W. Sari, "Study of Lysine and Asparagine as Capping Agent for Gold Nanoparticles," *Journal of Physics: Conference Series*, vol. 2243, no. 1, p. 012102, 2022/06/01 2022, doi: 10.1088/1742-6596/2243/1/012102.
 27. O. Horovitz et al., "Lysine Mediated Assembly of Gold Nanoparticles," *Studia Universitatis Babes-Bolyai Chemia*, vol. 52, pp. 97-108, 01/01 2007.
 28. M. Muhammad Mailafiya et al., "Evaluation of In-Vitro Release Kinetic and Mechanisms of Curcumin Loaded-Cockle Shell-Derived Calcium Carbonate Nanoparticles," 2019.
 29. E. E. Eltamany et al., "A New Saponin (Zygo-albuside D) from *Zygophyllum album* Roots Triggers Apoptosis in Non-Small Cell Lung Carcinoma (A549 Cells) through CDK-2 Inhibition," (in eng), *ACS Omega*, vol. 8, no. 33, pp. 30630-30639, Aug 22 2023, doi: 10.1021/acsomega.3c04314.
 30. S. Zhang, Y. Geng, N. Ye, and Y. Xiang, "A simple and sensitive colorimetric sensor for determination of gentamicin in milk based on lysine functionalized gold nanoparticles," *Microchemical Journal*, vol. 158, p. 105190, 2020/11/01/ 2020, doi: <https://doi.org/10.1016/j.microc.2020.105190>.
 31. H. P. Lestari, S. Martono, R. Wulandari, and A. Rohman, "Simultaneous analysis of Curcumin and demethoxycurcumin in Curcuma xanthorrhiza using FTIR spectroscopy and chemometrics," *International Food Research Journal*, vol. 24, no. 5, pp. 2097-2101, 2017.
 32. P. Vale, "Effects of light quality and nutrient availability on accumulation of mycosporine-like amino acids in *Gymnodinium catenatum* (Dinophyceae)," *Journal of photochemistry and photobiology. B, Biology*, vol. 143, pp. 20-9, 2015.
 33. A. M. Al-Roumy et al., "Nonlinear Optical Properties and All Optical Switching of Curcumin Derivatives," *Journal of Fluorescence*, vol. 34, no. 1, pp. 283-303, 2024/01/01 2024, doi: 10.1007/s10895-023-03257-5.
 34. K. Hazra et al., "Uv-Visible Spectrophotometric Estimation Of Curcumin In Nanoformulation," *International Journal of Pharmacognosy*, vol. 2, pp. 127-130, 01/01 2015, doi: 10.13040/IJPSR.0975-8232.IJP.2(3).127-30.
 35. M. L. Lestari and G. Indrayanto, "Curcumin," (in eng), *Profiles Drug Subst Excip Relat Methodol*, vol. 39, pp. 113-204, 2014, doi: 10.1016/b978-0-12-800173-8.00003-9.
 36. S. Mondal, S. Ghosh, and S. P. Moulik, "Stability of curcumin in different solvent and solution media: UV-visible and steady-state fluorescence spectral study," (in eng), *J Photochem Photobiol B*, vol. 158, pp. 212-8, May 2016, doi: 10.1016/j.jphotobiol.2016.03.004.
 37. Prasad V Kadam, Kavita N Yadav, Chandrashekhara L Bhingare, and M. J. Patil., "Standardization and quantification of curcumin from *Curcuma longa* extract using UV visible spectroscopy and HPLC.," *Journal of Pharmacognosy and Phytochemistry*, vol. 7, no. 5, pp. 1913-1918, 2018.
 38. Y. B. Murti, Y. S. Hartini, W. L. Hinrichs, H. W. Frijlink, and D. Setyaningsih, "UV-Vis spectroscopy to enable determination of the dissolution behavior of solid dispersions containing curcumin and piperine," *Journal of Young Pharmacists*, vol. 11, no. 1, p. 26, 2019.
 39. V. Joice and P. Metilda, "Synthesis, characterization and biological applications of curcumin-lysine based Schiff base and its metal complexes," *Journal of Coordination Chemistry*, vol. 74, pp. 2395-2406, 07/18 2021, doi: 10.1080/00958972.2021.1951258.
 40. A. Gupta, S. Mahajan, and R. Sharma, "Evaluation of antimicrobial activity of *Curcuma longa* rhizome extract against *Staphylococcus aureus*," (in eng), *Biotechnol Rep (Amst)*, vol. 6, pp. 51-55, Jun 2015, doi: 10.1016/j.btre.2015.02.001.
 41. K. Gurning, "Antimicrobial Activity of Ethanol Extract of Rhizome Turmeric (*Curcuma Longa* L.) For Growth of *Escherichia coli*, *Staphylococcus aureus* and *Candida albicans*," *Asian Journal of Pharmaceutical Research and Development*, vol. 8, pp. 5-8, 06/15 2020, doi: 10.22270/ajprd.v8i3.712.
 42. S. S. Hettiarachchi, Y. Perera, S. P. Dunuweera, A. N. Dunuweera, S. Rajapakse, and R. M. G. Rajapakse, "Comparison of Antibacterial Activity of Nanocurcumin with Bulk Curcumin," (in eng), *ACS Omega*, vol. 7, no. 50, pp. 46494-46500, Dec 20 2022, doi: 10.1021/acsomega.2c05293.
 43. S. Mukhtar and I. Ghori, "Antibacterial activity of aqueous and ethanolic extracts of garlic, cinnamon and turmeric against *Escherichia coli* ATCC 25922 and *Bacillus subtilis* DSM 3256," *International Journal of Applied Biology and Pharmaceutical Technology*, vol. 3, no. 2, pp. 131-136, 2012.
 44. S. Shahi et al., "Broad Spectrum Herbal Therapy against Superficial Fungal Infections," *Skin pharmacology and applied skin physiology*, vol. 13, pp. 60-4, 02/01 2000, doi: 10.1159/000029909.
 45. Y.-Q. Li, Q. Han, J.-L. Feng, W.-L. Tian, and H.-Z. Mo, "Antibacterial characteristics and mechanisms of ϵ -poly-lysine against *Escherichia coli* and *Staphylococcus aureus*," *Food Control*, vol. 43, pp. 22-27, 2014/09/01/ 2014, doi: <https://doi.org/10.1016/j.foodcont.2014.02.023>.

46. Z. Tan, Y. Shi, B. Xing, Y. Hou, J. Cui, and S. Jia, "The antimicrobial effects and mechanism of ϵ -poly-lysine against *Staphylococcus aureus*," *Bioresources and Bioprocessing*, vol. 6, no. 1, p. 11, 2019/04/13 2019, doi: 10.1186/s40643-019-0246-8.
47. A. Vibhute et al., "Fluorescent Carbon Quantum Dots Functionalized by Poly L-Lysine: Efficient Material for Antibacterial, Bioimaging and Antiangiogenesis Applications," *Journal of Fluorescence*, vol. 32, no. 5, pp. 1789-1800, 2022/09/01 2022, doi: 10.1007/s10895-022-02977-4.
48. V. Xuan Hoa, T. Duong, T. Pham, D. Trinh, X. Nguyen, and V.-S. Dang, "Synthesis and study of silver nanoparticles for antibacterial activity against *Escherichia coli* and *Staphylococcus aureus*," *Advances in Natural Sciences: Nanoscience and Nanotechnology*, vol. 9, p. 025019, 06/08 2018, doi: 10.1088/2043-6254/aac58f.
49. Pradeepa, S. M. Vidya, S. Mutalik, K. Udaya Bhat, P. Huilgol, and K. Avadhani, "Preparation of gold nanoparticles by novel bacterial exopolysaccharide for antibiotic delivery," *Life Sciences*, vol. 153, pp. 171-179, 2016/05/15/ 2016, doi: <https://doi.org/10.1016/j.lfs.2016.04.022>.